

Structural Analysis and Identity Confirmation of Anthocyanins in *Brassica oleracea* Extracts by Direct Injection Ion Mobility-Mass Spectrometry

River J. Pachulicz, Long Yu, Blagojce Jovceviski, Vincent Bulone, and Tara L. Pukala*

Cite This: *ACS Meas. Sci. Au* 2023, 3, 200–207

Read Online

ACCESS |

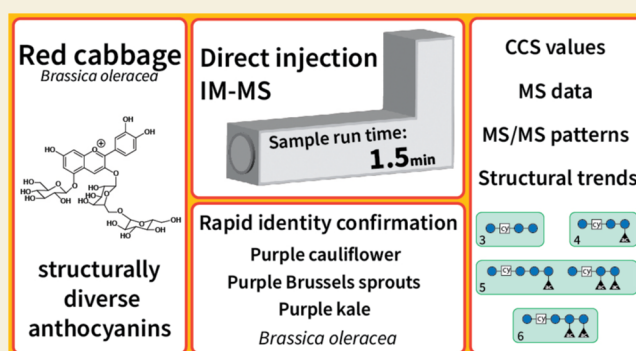
Metrics & More

Article Recommendations

Supporting Information

ABSTRACT: Anthocyanins are a subclass of plant-derived flavonoids that demonstrate immense structural heterogeneity which is challenging to capture in complex extracts by traditional liquid chromatography–mass spectrometry (MS)-based approaches. Here, we investigate direct injection ion mobility-MS as a rapid analytical tool to characterize anthocyanin structural features in red cabbage (*Brassica oleracea*) extracts. Within a 1.5 min sample run time, we observe localization of structurally similar anthocyanins and their isobars into discrete drift time regions based upon their degree of chemical modifications. Furthermore, drift time-aligned fragmentation enables simultaneous collection of MS, MS/MS, and collisional cross-section data for individual anthocyanin species down to a low picomole scale to generate structural identifiers for rapid identity confirmation. We finally identify anthocyanins in three other *Brassica oleracea* extracts based on red cabbage anthocyanin identifiers to demonstrate our high-throughput approach. Direct injection ion mobility-MS therefore provides wholistic structural information on structurally similar, and even isobaric, anthocyanins in complex plant extracts, which can inform the nutritional value of a plant and bolster drug discovery pipelines.

KEYWORDS: ion mobility-mass spectrometry, anthocyanins, *Brassica oleracea*, rapid profiling, identity confirmation, structural analysis



1. INTRODUCTION

Plants contain an enormous pool of phytochemicals that exhibit unique chemical structures and diverse biological activities. For example, polyphenols are a class of secondary phytochemicals defined by multiple phenol groups in their structure, with documented ameliorative effects on long-term human health.¹ Among polyphenols are a subclass of flavonoids called anthocyanins; pigments that impart red, blue, and purple hues to plant tissues. Anthocyanins exhibit diverse bioactive properties both *in vitro* and *in vivo* including neuroprotective, antimicrobial, and radical scavenging effects and have been commercially utilized in nutraceuticals and as natural food colorants.^{2–6}

Composed of a 2-phenylbenzopyrylium ion core, denoted an anthocyanidin, anthocyanins are glycosylated and/or acylated forms of anthocyanidins. Due to the distinct number of sugar and aliphatic/aromatic acyl substituents that can modify various positions of the anthocyanidin core, anthocyanins display vast structural heterogeneity, with naturally occurring isobaric and structural isomers being common.⁷ Ion mobility-mass spectrometry (IM-MS) is a powerful tool that captures the structural complexity of these compounds by the separation of individual species based on their shape or collisional cross-section (CCS).⁸ This technique hence can

distinguish between discrete structural isomers, which have identical mass-to-charge ratios (m/z) but different three-dimensional (3D) structures, with even the epimers cyanidin-3-galactose and cyanidin-3-glucose resolvable.^{7,9}

Analysis of anthocyanins in plant extracts typically involves coupling liquid chromatography to diode array detection (LC-DAD) and mass spectrometry (LC-DAD-MS), whereby optical absorbance is used for classification and quantification of individual anthocyanin species as identified by MS.¹⁰ These approaches provide simultaneous retention time and spectroscopic information for all observable species present, and, for this reason, have been used to elucidate the anthocyanin composition of countless plant extracts.^{11–14} However, such analyses often rely on sample-dependent LC optimization, which can drastically increase sample run times, leading to an overall reduction in the throughput of analysis. LC-DAD-MS

Received: October 13, 2022

Revised: January 29, 2023

Accepted: January 30, 2023

Published: February 9, 2023



approaches also yield limited structural information and hence, when profiling complex extracts that contain classes of compounds with similar structural features, such approaches are unable to elucidate clear structural trends.

Previous investigation of anthocyanins and other polyphenolic components of plant extracts by IM-MS typically involves coupling to liquid chromatography (LC).¹⁵ Here, we demonstrate direct injection IM-MS as a tool for rapid anthocyanin characterization of *Brassica oleracea* extracts which are known to contain multiple, structurally similar anthocyanin compounds. Analysis of red cabbage extracts by traditional LC-DAD-MS indicated prevalent coelution of similar anthocyanin structures, making identification of structural trends challenging. However, by direct injection IM-MS, we successfully visualize distinct anthocyanin structural trends based on their degree of modification and observe the separation of isobaric anthocyanin species. Drift time-aligned fragmentation generates indicative fragmentation patterns simultaneously for all anthocyanins present, which can be used in structure identification. Furthermore, we begin constructing a library of red cabbage anthocyanin CCS values, which we use to perform rapid identity confirmation in other *Brassica oleracea* extracts. Our work highlights direct injection IM-MS as a high-throughput analytical tool to characterize the phytochemical composition of plant extracts to inform their nutritional value.

2. MATERIALS AND METHODS

2.1. Preparation of Anthocyanin-Enriched Extracts

Red cabbage, purple kale, purple Brussels sprouts, and purple cauliflower (500 g each) were purchased from local supermarkets in Adelaide, Australia, in 2021. Samples of red cabbage, purple kale, purple Brussels sprouts and purple cauliflower were prepared as outlined previously.¹¹ Briefly, the lyophilized plant material was extracted twice at room temperature with 2% aqueous formic acid (FA), with the supernatants collected and combined after centrifugation. The supernatants were then loaded onto an Amberlite XAD7HP resin (Sigma Aldrich, St. Louis, USA) and washed with 2% aqueous FA to remove unbound compounds and then with 2% FA in methanol to elute the remaining anthocyanins. The eluates were dried under N₂, redissolved in 2% aqueous FA, and lyophilized to yield anthocyanin-enriched extracts of each plant.

2.2. Analysis of Red Cabbage Extract by LC-DAD-MS

Red cabbage extracts were dissolved in 2% aqueous FA (1 mg/mL) and analyzed using an Agilent 1260 Infinity LC coupled to an Agilent 1290 Infinity II Diode Array Detector and an Agilent 6495B Triple Quadrupole in a HPLC-DAD-QQQ platform (Agilent Technologies, Santa Clara, USA) as described previously.¹¹ Briefly, red cabbage extract (5 μ L) was injected and passed through an Agilent Poroshell 120 SB-C18 column (100 mm \times 2.1 mm \times 2.7 μ m) (Agilent Technologies, Santa Clara, USA) at a flow rate of 0.3 mL min⁻¹. DAD detection was set at 520 nm. MS detection was conducted in positive mode using an AJS ESI source. All data were processed with MassHunter Qualitative and Quantitative analysis 10.0 (Agilent Technologies, Santa Clara, USA).

2.3. Analysis of *Brassica oleracea* Extract by Direct Injection IM-MS

IM-MS analysis of *Brassica oleracea* extracts dissolved in 2% aqueous FA (1 mg/mL) was performed on an Agilent 6560 IM-QTOF platform (Agilent Technologies, Santa Clara, USA). The sample (5 μ L) was injected and electrosprayed using 50% aqueous acetonitrile containing 0.01% FA at a flow rate of 0.1 mL/min, without chromatographic separation. The experimental setup for the detection of anthocyanins by MS was as follows: dual AJS ESI source in positive mode, N₂ drying gas temperature and flow 300 °C and 8 L/min

respectively, nebulizer 30 psi; sheath gas temperature and flow 300 °C and 12 L/min respectively, capillary and nozzle voltage 3500 and 500 V respectively. Data were collected with a frame rate of 1 and a scan range of 100–3200 *m/z*. Parameters for the drift tube were as follows: N₂ as the collision gas, trap fill time 5000 μ s, trap release time 150 μ s, IM transient rate of 16, drift tube entrance voltage 1700 V, drift tube exit voltage 250 V, and drift tube pressure 3.94 Torr. Each extract was run in an alternating frame fragmentation scheme whereby fragmentation occurs after IM separation at alternating low and high collision energies. Low collision energy frames were conducted at 0 V while high energy collision frames were conducted in repeated experiments at increasing 5 V collision energy increments (15–45 V) to collect MS/MS fragmentation data for anthocyanins. Single-field CCS calculations were processed in IM-MS Browser (v.10.0, Agilent Technologies, Santa Clara, USA) using the Agilent ESI Tune Mix as the reference set.^{16,17}

3. RESULTS AND DISCUSSION

3.1. Analysis of Red Cabbage Extract by LC-DAD-MS Demonstrates the Co-Elution of Structurally Similar Anthocyanin Species and Provides Limited Structural Information

Red cabbage anthocyanins are known to be a complex assortment of structurally similar species. Consisting of a characteristic cyanidin-3-diglucoside-5-glucoside scaffold, a variety of caffeic, p-coumaric, sinapic, and ferulic acid acyl partners typically modify the 3-C glucosyl units to yield structurally diverse anthocyanins.^{18–20} Figure 1 summarizes the general scaffold of anthocyanin structures in *Brassica oleracea*. Capturing the structural complexity of these compounds can be challenging, with extensive LC optimization

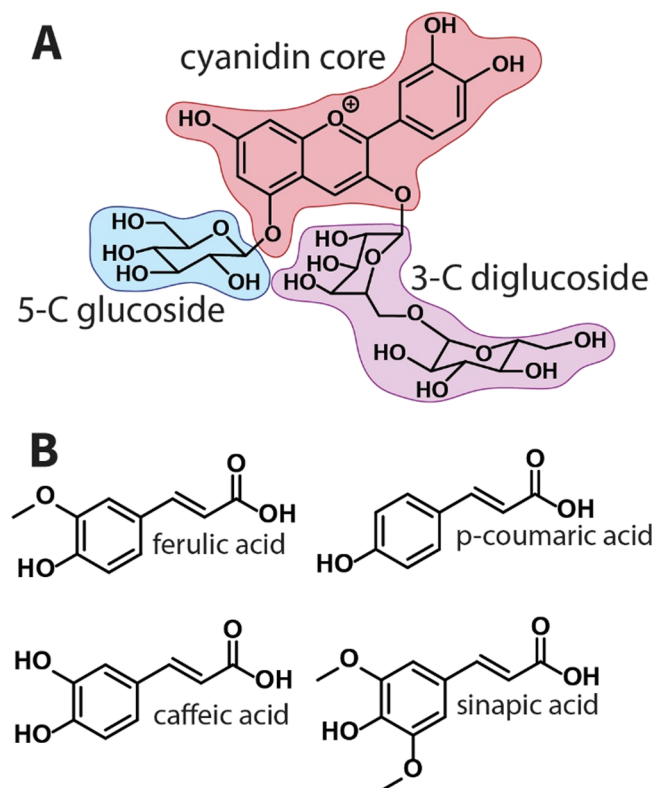


Figure 1. *Brassica oleracea* anthocyanin structural features. General cyanidin-3-diglucoside-5-glucoside structure (A) with possible aromatic acyl substituents that typically modify the 3-C glucosyl units (B).

first needed to provide the greatest separation of the various structural forms.

Red cabbage extract was first analyzed for reference by a standard LC-DAD-MS approach, with the corresponding chromatographic trace at 520 nm shown in Figure 2. The

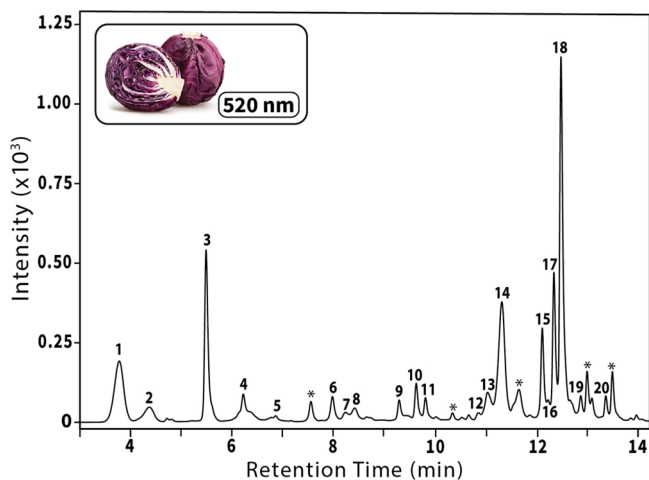


Figure 2. LC-DAD-MS chromatographic trace of a red cabbage extract at 520 nm. Peaks containing identified anthocyanins are labeled 1–20 (*peaks which contained compounds that could not be identified).

identification of anthocyanins present in each peak was conducted with reference to the literature and by matching m/z values, fragmentation patterns, and retention times. The anthocyanins identified in red cabbage extract by LC-DAD-MS are summarized in Table 1. The analysis of red cabbage extract at 520 nm showed 20 peaks containing previously identified anthocyanins, with many containing multiple co-eluting anthocyanin species.^{18–22} For example, the chromatographic peak at 11.34 min (peak #14 in Figure 2) showed co-elution of two structurally similar anthocyanins, cyanidin-3-feruloyldigluco-5-glucoside (m/z 949) and cyanidin-3-sinapoyldigluco-5-glucoside (m/z 979). Separation of these individual species by LC has been achieved previously, however; this separation increased sample run time to over an hour.²¹ This co-elution effect was also seen in peaks 3, 5, 6, 10, 11, and 13 (Figure 2), which together comprised approximately one third of the total anthocyanin content based on the peak area.

Visualizing structural trends or patterns among red cabbage anthocyanins by LC-based methods is difficult, mostly due to the highly conserved structural modifications that are seen in their structures. The anthocyanins with m/z 1125, 1155, and 1185 are diacylated derivatives of cyanidin-3-digluco-5-glucoside, containing diferuloyl, feruloylsinapoyl, and disinapoyl modifications, respectively, explaining the subsequent mass increases of 30 Da across these species. The identification of such structural relationships can be inferred with LC–MS data, but they can be hard to definitively visualize, especially when many structurally related species are present. Additionally, the ability to quantify the individual abundances of each

Table 1. Anthocyanin Species Identified by LC-DAD-MS in Red Cabbage Extract^a

Peak Number	Retention Time (min)	Anthocyanin	[M] ⁺ (m/z)	MS/MS (m/z)
1	3.78	cyanidin-3-digluco-5-glucoside	773	611/449/287
2	4.38	cyanidin-3-caffeoyl-p-coumaroyldigluco-5-glucoside	1081	919/449/287
3	5.50	cyanidin-3-sinapoyltrigluco-5-glucoside/cyanidin-3-caffeoylsinapoyldigluco-5-glucoside*	1141	979/449/287
		cyanidin-3-feruloyldigluco-5-glucoside	949	787/449/287
4	6.23	cyanidin-3-sinapoyldigluco-5-glucoside	979	817/449/287
5	6.87	cyanidin-3-sinapoyldigluco-5-glucoside	979	817/449/287
		cyanidin-3-p-coumaroyldigluco-5-glucoside	919	757/449/287
6	7.99	cyanidin-3-caffeoyl-p-coumaroyldigluco-5-glucoside	1081	919/449/287
		cyanidin-3-sinapoyldigluco-5-glucoside	979	817/449/287
7	8.25	cyanidin-3-feruloyltrigluco-5-glucoside/cyanidin-3-caffeoylferuloyldigluco-5-glucoside*	1111	949/449/287
8	8.43	cyanidin-3-sinapoyltrigluco-5-glucoside/cyanidin-3-caffeoylsinapoyldigluco-5-glucoside*	1141	979/449/287
9	9.31	cyanidin-3-diferuloyltrigluco-5-glucoside	1287	1125/449/287
10	9.65	cyanidin-3-feruloylsinapoyltrigluco-5-glucoside	1317	1155/449/287
		cyanidin-3-caffeoyldigluco-5-glucoside	935	773/449/287
11	9.83	cyanidin-3-disinapoyltrigluco-5-glucoside	1347	1185/449/287
		cyanidin-3-feruloyltrigluco-5-glucoside/cyanidin-3-caffeoylferuloyldigluco-5-glucoside*	1111	949/449/287
12	10.88	cyanidin-3-p-coumaroyldigluco-5-glucoside	919	757/449/287
13	11.058	cyanidin-3-sinapoyltrigluco-5-glucoside/cyanidin-3-caffeoylsinapoyldigluco-5-glucoside*	1141	979/449/287
		cyanidin-3-p-coumaroyldigluco-5-glucoside	919	757/449/287
14	11.34	cyanidin-3-sinapoyldigluco-5-glucoside	979	817/449/287
		cyanidin-3-feruloyldigluco-5-glucoside	949	787/449/287
15	12.14	cyanidin-3-diferuloyldigluco-5-glucoside	1125	963/449/287
16	12.25	unknown	1171	1009/449/287
17	12.37	cyanidin-3-feruloylsinapoyldigluco-5-glucoside	1155	993/449/287
18	12.51	cyanidin-3-disinapoyldigluco-5-glucoside	1185	1023/449/287
19	12.90	cyanidin-3-p-coumaroyldigluco-5-malonylglucoside	1005	757/535/287
20	13.39	cyanidin-3-feruloylsinapoyldigluco-5-glucoside	1155	993/449/287

^aAnthocyanins found in each peak with their corresponding retention time (min), MS data (m/z), and MS/MS patterns. (*Anthocyanins where different isobaric structures have been previously identified but were not distinguishable.)

anthocyanin is made difficult by the lack of resolution we see in our LC separation. Hence, approaches that circumvent the difficulties associated with LC–MS workflows would thus be useful in characterizing the chemical and structural complexity of plant extracts.

3.2. Analysis of a Red Cabbage Extract by Direction Injection IM-MS Provides Wholistic Structural Information on Individual Anthocyanin Species and Their Isobars

IM-MS is a powerful analytical tool that separates gas phase ions by their mass, charge, and shape. This three-dimensional separation can allow for structurally similar compounds that are challenging to resolve by conventional methods such as LC to be separated. IM-MS can be applied to anthocyanins in plant extracts to better visualize anthocyanin structural trends and map individual species. Furthermore, with IM separation taking place on the millisecond time scale, it offers a dramatic advantage to throughput of experimental analysis.

Red cabbage extract was next analyzed by direct injection IM-MS on an Agilent 6560 IMQTOF for comparison to LC-DAD-MS identification, as described in Section 3.1, with the IM-MS data shown in Figure 3A. The corresponding m/z values, drift times, and CCS data for observable anthocyanins is summarized in Table 2. CCS values are a physical measurement related to an ions' 3D shape that can be used as a unique identifier for any given compound. The CCS values presented here were measured through drift-time ion mobility, which provides accurate, direct CCS measurements for all observable ions in a sample.

To visualize structural trends by IM-MS, we adopted an all-ion fragmentation approach to rapidly identify the anthocyanins in red cabbage extract. This involves acquisition of alternating high and low energy IM-MS scans to collect both precursor and fragmentation data for all analytes present. As seen in Figure 3B, because fragmentation occurs post-separation by IM, fragments of each anthocyanin appear at identical drift times as the precursor ion. Signals at m/z 287 and 449 in high energy scans, which correspond to cyanidin and cyanidin-3-glucoside, are conserved fragments in *Brassica oleracea* anthocyanins and hence can be used to infer the presence of these compounds. Optimization of fragmenting voltages was conducted, and it was found that 35 V successfully showed characteristic fragmentation for all anthocyanin species in the extract simultaneously.

By direct injection IM-MS, the majority of anthocyanins identified by LC-DAD-MS, summarized in section 3.1, had observable signals. However, signal loss for anthocyanins with m/z 935 and 1005 occurred. As expected with adopting high-throughput approaches, a trade-off between sensitivity and sample run time must be made. Despite our approach being unable to capture compounds in trace amounts, we are still able to detect the major anthocyanin components of red cabbage extract while reducing the sample analysis time 16-fold, from 24 to 1.5 min. In other words, by our IM-MS approach, we have an hourly sample analysis turnover of 40 whereas only 2 samples could be analyzed by our LC-DAD-MS approach. Hence, our approach shows minor signal loss compared to the great reduction in sample run time we achieve.

As seen in Figure 3A, clear trends in the drift time distribution and m/z values of individual anthocyanin species in red cabbage extract are observed, which are related to their respective degrees of structural modifications. For example, m/z

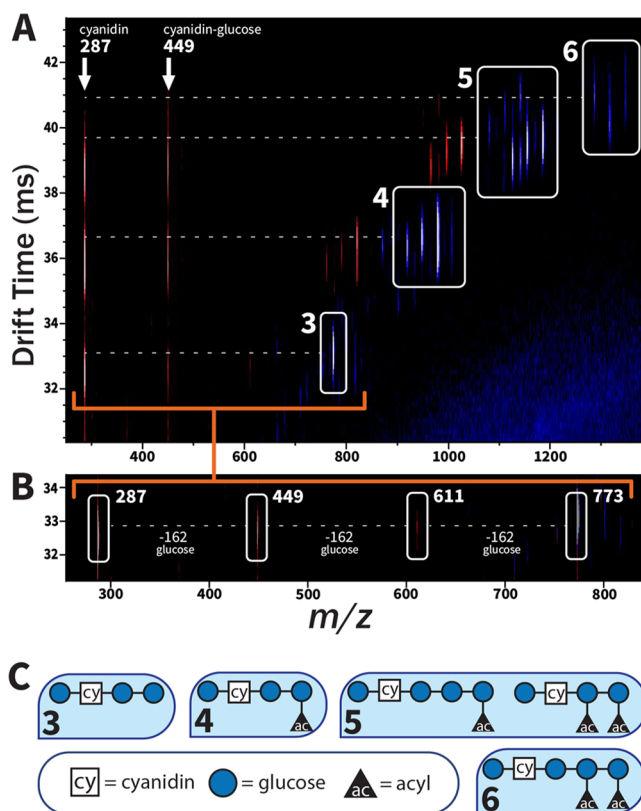


Figure 3. Ion mobility plot of a red cabbage extract analyzed by direct injection IM-MS. (A) Low voltage collision energy (0 V) results are shown in blue, whereas high voltage collision energy (35 V) results are shown in red. Fragments of each anthocyanin are drift-time aligned to their precursor ion as fragmentation occurs after IM separation. Discrete drift time distributions of structurally related anthocyanins are outlined by white boxes and are labeled with values based on the number of structural modifications they exhibit. The fragments m/z 287 and m/z 449 corresponding to cyanidin and cyanidin-3-glucoside are labeled with their corresponding sets of precursor ions. (B) Zoomed in fragmentation of cyanidin-3-diglucoside-5-glucoside (m/z 773) with each fragment labeled with their respective m/z . (C) General anthocyanin structural patterns for each level of modification. Numbering (3, 4, 5, 6) corresponds to the numbering of white boxes shown in Figure 3A.

m/z 773 is cyanidin-3-diglucoside-5-glucoside, which contains three structural modifications, in this case being three glucosyl residues. As no other anthocyanins identified in this extract exhibit only three structural modifications, its drift time occurs shorter than all other anthocyanins at around 33.1 ms. Conversely, the compounds with m/z 919, 949, and 979 each contain four distinct structural modifications, being different combinations of glucosyl and acyl groups, yielding an average drift time of 36.3 ms. This trend also applied for the compounds with m/z 1111, 1125, 1141, 1155, 1171, and 1185, each containing five structural modifications with an average drift time of 39.6 ms and m/z 1287, 1317, and 1347, each containing six structural modifications with an average drift time of 40.6 ms. A general summary of these structural patterns is depicted in Figure 3C. This distinct trend of red cabbage anthocyanins separating into specific drift time regions based upon their respective structural modifications makes it possible to predict or infer the general structure of unknown or novel anthocyanins in future.

Table 2. Anthocyanin Species Characterized in Red Cabbage Extract by Direct Injection IM-MS^a

Anthocyanin	[M] ⁺ (<i>m/z</i>)	Drift Time (ms)	^{DT} CCS _{N₂} (±SD)
cyanidin-3-diglucoside-5-glucoside	773.214	33.1	275.6 (0.1)
cyanidin-3-p-coumaroyldiglucoside-5-glucoside	919.251	36.3	302.3 (0.1)
cyanidin-3-feruloyldiglucoside-5-glucoside	949.262	36.2	301.1 (5.3)
cyanidin-3-sinapoyldiglucoside-5-glucoside	979.272	36.5	303.0 (0.2)
cyanidin-3-caffeoyl-p-coumaroyldiglucoside-5-glucoside	1081.283	40.0	332.2 (0.2)
cyanidin-3-caffeoylferuloyldiglucoside-5-glucoside/cyanidin-3-feruloyltrigluco- sideside*	1111.308	38.9	322.9 (1.6)
	1111.308	40.5	336.8 (0.2)
cyanidin-3-diferuloyldiglucoside-5-glucoside	1125.308	39.5	328.3 (5.7)
cyanidin-3-caffeoylsinapoyldiglucoside-5-glucoside/cyanidin-3-sinapoyltrigluco- sideside*	1141.323	39.0	323.9 (0.1)
	1141.323	41.0	340.5 (0.2)
cyanidin-3-feruloylsinapoyldiglucoside-5-glucoside	1155.320	39.5	327.7 (0.1)
unknown	1171.327	39.7	329.8 (1.0)
cyanidin-3-disinapoyldiglucoside-5-glucoside	1185.331	39.7	329.4 (0.1)
cyanidin-3-diferuloyltrigluco- sideside	1287.364	41.1	340.6 (0.2)
cyanidin-3-feruloylsinapoyltrigluco- sideside	1317.360	40.2	333.0 (0.2)
cyanidin-3-disinapoyltrigluco- sideside	1347.361	40.7	337.5 (0.3)

^aAll observable anthocyanins with their corresponding drift times, MS data (*m/z*), calculated CCS values, and CCS sample standard deviations for technical replicates of the same extract (*n* = 3). (*Anthocyanins where different isobaric structures have been previously identified but were not distinguishable.)

In addition to the separation of anthocyanins by their degree of structural modification, multiple signals at *m/z* 1111 and 1141 are observed, corresponding to distinct isobaric forms of these species, with arrival time distributions for these compounds shown in Figure S2. Based on the previous literature, two assignments have been made for *m/z* 1141, being cyanidin-3-sinapoyltrigluco-5-glucoside and cyanidin-3-caffeoylsinapoyldiglucoside-5-glucoside.²² Additionally, two assignments have been made for *m/z* 1111, being cyanidin-3-feruloyltrigluco-5-glucoside and cyanidin-3-caffeoylferuloyldiglucoside-5-glucoside, which yield a 30 Da decrease to their structurally related *m/z* 1141 counterparts, due to a sinapic acid group exchanged for a ferulic acid group. Although we could not resolve the mass differences between these isobars, with supporting in silico evidence as well as using anthocyanins standards, it would be possible to confidently assign each isobaric structure to its corresponding drift time signal. These structural trends and isobaric anthocyanins are hence easily observed by IM-MS, whereas their identification using typical LC-based approaches would be challenging.

We compared our direct injection IM-MS approach to both LCQTOF and direct injection QTOF methods to highlight the advantages of using IM over using QTOF approaches alone. Red cabbage extracts were analyzed by LCQTOF and direct injection QTOF with the data shown in Figure S1. By direct injection QTOF, *m/z* peaks for all anthocyanins identified by LC-DAD-MS were observed. However, it is not possible to clearly determine the presence of isobaric species without some other degree of separation. Furthermore, no 3D information is obtained, and hence, structural investigation of anthocyanins by direct injection QTOF is not possible. These issues are largely the same for the LCQTOF analysis of red cabbage extracts, with limited structural information on anthocyanin species able to be collected. This demonstrates the advantages of coupling IM analysis to QTOF platforms, which include detecting isobaric species and investigating structural relationships.

We assessed the limit of detection (LOD) for our IM-MS approach by the addition of malvidin-3-glucoside anthocyanin (*m/z* 493.133) as an internal standard into our red cabbage

extract, with an observed detection threshold of 0.5 μM, equating to 2.5 pmol (1.23 ng). To investigate the reason for the loss in sensitivity in our IM-MS approach, we compared LODs across different experimental platforms (Table S1). LC-DAD-MS and direct injection IM-MS showed identical LODs (1.23 ng) with direct injection QTOF and LC-QTOF showing lower LODs, respectively (123 and 12 pg). We rationalize that the loss in sensitivity observed in our IM-MS approach is likely due to a combination of ion suppression through direct injection into the MS and loss of ions in the drift tube, which will have a more noticeable effect on the least abundant species in red cabbage extract, which we observed for anthocyanins *m/z* 935 and 1005. However, we are still able to detect the major anthocyanin component in a complex extract while greatly reducing analysis time, showing that our approach can still give meaningful insight into the nutritional functionality of a plant extract in addition to its chemical composition. With further optimization and appropriate isotopically labeled standards, it will be possible to perform simultaneous quantification of each observable anthocyanin down to a low picomole scale by our IM-MS approach.

The data shown in Figure 3A were collected in 1.5 min and provide expansive structural information for a complex mixture of structurally related compounds. This approach is well suited to not only study anthocyanins in a range of plant extracts but also other classes of polyphenolic compounds that have great structural heterogeneity and relatively simple fragmentation patterns. Even within Figure 3A, we can observe other non-anthocyanin signals likely corresponding to other polyphenolic compounds retained in our anthocyanin-enriching procedure. Hence, it is possible to characterize the whole polyphenolic composition of a plant extract in this approach if comprehensive information on the various classes of compounds being analyzed is known. Direct injection IM-MS therefore provides a high-throughput, structurally comprehensive method to categorize and profile anthocyanins in plant extracts without the need for LC optimization.

3.3. Rapid Identity Confirmation of Anthocyanins in *Brassica oleracea* Extracts by CCS and *m/z*

Having demonstrated the power of direct injection IM-MS to structurally identify anthocyanins in red cabbage extracts, we sought to rapidly identify anthocyanins in other *Brassica oleracea* extracts using their *m/z* and CCS values. Anthocyanin-enriched extracts from purple cauliflower, purple kale, and purple Brussels sprouts were analyzed by direct injection IM-MS, with the ion mobility plots of each extract found in Figure S3. Identity confirmation of anthocyanins in these extracts was conducted by comparison to the small anthocyanin CCS and *m/z* library developed in Section 3.2. The anthocyanins identified in each extract by this method are listed in Table 3.

Across the three additional *Brassica oleracea* extracts tested, nine anthocyanin species were identified by comparison to red cabbage anthocyanin CCS and *m/z* measurements. All CCS measurements for matching anthocyanins in purple cauliflower, purple kale, and purple Brussels sprouts obtained by direct injection IM-MS were within a 2% error range for those collected in red cabbage, as expected for our experimental setup.²³ These nine species had been previously characterized across multiple *Brassica oleracea* extracts, successfully demonstrating the rapid identity confirmation of anthocyanins by *m/z* and CCS.^{19,24,25} It is well established that these other *Brassica oleracea* extracts contain diverse anthocyanin structures that are not present in red cabbage; hence, by this method, we are not able to capture the full complexity of these extracts simultaneously.^{19,24,25} However, the development of a more extensive database of CCS values for various anthocyanin species across a range of plant extracts and synthetic standards will allow for greatly expanded and comprehensive identity confirmation of the whole anthocyanin profile of a particular biomass. This can further be extended to other classes of polyphenolic compounds to develop a high-throughput, structurally informative approach to capturing the complex polyphenolic profile of a plant extract.

4. CONCLUDING REMARKS

LC-DAD-MS approaches have long been used to characterize anthocyanin profiles in plant extracts. Such approaches often prove challenging in cases where many structurally similar compounds are present, whereby the co-elution of individual species can persist even after extensive LC optimization. Additionally, structural trends among these compounds are difficult to discern by these approaches, and hence, employing novel analytical tools to visualize structural relationships can inform on the properties and applications of these compounds.

We demonstrate the ability of direct injection IM-MS to yield comprehensive structural information on a complex mixture of structurally similar anthocyanins abundant in red cabbage. We not only separate structurally similar anthocyanins which co-eluted by LC analysis but we also separate isobaric anthocyanins with identical nominal masses. Drift time distribution trends among anthocyanins based on their degree of structural modification were observed, which can be used to predict the general structural features of novel or unknown anthocyanins. Furthermore, simultaneous activation of all anthocyanins post-IM separation yielded conserved fragmentation patterns that can be used to infer the presence of anthocyanins in a plant extract.

Finally, we have begun the construction of a CCS library for anthocyanins identified in red cabbage to undertake the rapid

Table 3. Identity Confirmation of Anthocyanins in *Brassica oleracea* Extracts Based upon Red Cabbage Anthocyanin CCS Values^a

anthocyanin	[M] ⁺ (<i>m/z</i>)	red cabbage		purple kale		purple brussels sprouts		purple cauliflower	
		CCS (± SD)	% Error	CCS (± SD)	% Error	CCS (± SD)	% error	CCS (± SD)	% Error
cyanidin-3-diglucoside-5-glucoside	773.214	275.6 (0.1)						275.0 (0.2)	-0.2
cyanidin-3-p-coumaroyldiglucoside-5-glucoside	919.251	302.3 (0.1)						301.7 (0.3)	-0.2
cyanidin-3-feruloyldiglucoside-5-glucoside	949.262	301.1 (5.3)	+0.9	303.9 (0.2)				305.4 (1.2)	+1.4
cyanidin-3-sinapoyldiglucoside-5-glucoside	979.272	303.0 (0.2)	-0.9	300.2 (0.2)				308.6 (1.4)	+1.8
cyanidin-3-diferuloyldiglucoside-5-glucoside	1125.308	328.3 (5.7)	-1.5	323.4 (0.1)					
cyanidin-3-caffeoylsinapoyldiglucoside-5-glucoside/cyanidin-3-sinapoyltriglucoside-5-glucoside*	1141.323	323.9 (0.1)	-0.3	322.8 (0.6)					
cyanidin-3-feruloylsinapoyldiglucoside-5-glucoside	1155.320	327.7 (0.1)	-0.2	327.2 (0.1)				327.2 (0.4)	-0.2
cyanidin-3-disinapoyldiglucoside-5-glucoside	1185.331	329.4 (0.1)	-0.4	328.1 (0.1)				328.7 (0.1)	-0.2
cyanidin-3-feruloylsinapoyltriglucoside-5-glucoside	1317.360	333.0 (0.2)	-0.2	332.4 (0.1)					

^aAnthocyanins in purple kale, purple Brussels sprouts, and purple cauliflower extracts identified by matching *m/z* and CCS (±SD (Sample)) values to those found in red cabbage. The percentage CCS error for each anthocyanin compared to that measured in red cabbage is also shown. Data are shown as the average of three technical triplicates. (*Anthocyanins where different isobaric structures have been previously identified but were not distinguishable.)

identity confirmation of anthocyanins in *Brassica oleracea* and other plant extracts. Nine anthocyanins were identified based on m/z and CCS measurements alone across purple cauliflower, purple Brussels sprouts, and purple kale extracts with data acquisition times less than 2 min. We therefore demonstrate a high-throughput, straightforward approach to capture the structural complexity of a plant extract by direct injection IM-MS.

Our work highlights the future potential of IM-MS as a powerful analytical tool to investigate and categorize the structural complexity of plant extracts, with a 16-fold reduction in analysis run time compared to traditional LC-DAD-MS approaches. Despite a caveat of decreased sensitivity compared to LC-DAD-MS workflows, direct injection IM-MS provides a robust, high-throughput method to analyze specific classes of phytochemicals down to a low picomole scale, which can help inform the biological properties or nutritional value of any biomass source. Improving the speed at which we can distinguish the metabolic features of a complex sample will prove critical in major industries such as drug discovery.

■ ASSOCIATED CONTENT

SI Supporting Information

The Supporting Information is available free of charge at <https://pubs.acs.org/doi/10.1021/acsmeasuresciau.2c00058>.

Data showing the analysis of red cabbage extract by direct injection QTOF and LCQTOF methods; ATD of isobaric anthocyanins species identified in red cabbage; LOD's for tested experimental methods; and IM-MS spectra of *Brassica oleracea* extracts and the anthocyanins identified by matching CCS and m/z values (PDF)

■ AUTHOR INFORMATION

Corresponding Author

Tara L. Pukala – Department of Chemistry, School of Physical Sciences, University of Adelaide, Adelaide, SA 5005, Australia; orcid.org/0000-0001-7391-1436; Email: tara.pukala@adelaide.edu.au

Authors

River J. Pachulicz – Department of Chemistry, School of Physical Sciences, University of Adelaide, Adelaide, SA 5005, Australia

Long Yu – School of Agriculture, Food and Wine, University of Adelaide, Adelaide, SA 5005, Australia

Blagojce Jovceviski – Department of Chemistry, School of Physical Sciences and School of Agriculture, Food and Wine, University of Adelaide, Adelaide, SA 5005, Australia; orcid.org/0000-0001-7999-1385

Vincent Bulone – School of Agriculture, Food and Wine, University of Adelaide, Adelaide, SA 5005, Australia; Division of Glycoscience, Department of Chemistry, School of Engineering Sciences in Chemistry, Biotechnology and Health, Royal Institute of Technology (KTH), AlbaNova, University Centre, Stockholm 106 91, Sweden; Present Address: College of Medicine and Public Health, Flinders University, Bedford Park Campus, Sturt Road, SA 5042, Australia

Complete contact information is available at: <https://pubs.acs.org/doi/10.1021/acsmeasuresciau.2c00058>

Author Contributions

R.J.P.: Conceptualization, Methodology, Investigation, Formal analysis, Writing - original draft, Writing - review & editing. L.Y.: Methodology, Investigation, Formal analysis, Writing - review & editing. B.J.: Methodology, Investigation, Formal analysis, Writing - review & editing. V.B.: Conceptualization, Methodology, Formal analysis, Writing - review & editing, Supervision. T.L.P.: Conceptualization, Methodology, Formal analysis, Writing - review & editing, Supervision. CRediT: **River Jack Pachulicz** conceptualization (equal), data curation (lead), formal analysis (lead), investigation (equal), methodology (equal), writing-original draft (lead), writing-review & editing (equal); **Long Yu** conceptualization (supporting), data curation (supporting), investigation (equal), methodology (equal), writing-review & editing (equal); **Blagojce Jovceviski** formal analysis (supporting), investigation (supporting), methodology (supporting), writing-review & editing (equal); **Vincent Bulone** conceptualization (equal), funding acquisition (lead), investigation (equal), methodology (equal), project administration (lead), resources (equal), supervision (equal), writing-review & editing (equal); **Tara L. Pukala** conceptualization (equal), formal analysis (supporting), funding acquisition (lead), investigation (supporting), methodology (equal), project administration (equal), supervision (equal), writing-review & editing (equal).

Notes

The authors declare no competing financial interest.

■ ACKNOWLEDGMENTS

R.J.P. is a recipient of an Australian Government Research Training Program stipend scholarship. This research was funded by the South Australian Department for Innovation and Skills via the Research Consortium for Agricultural Product Development (grant to V.B. and T.L.P.).

■ REFERENCES

- (1) Quideau, S.; Deffieux, D.; Douat-Casassus, C.; Pouységu, L. Plant polyphenols: Chemical properties, biological activities, and synthesis. *Angew. Chem., Int. Ed.* **2011**, *50*, 586–621.
- (2) Badshah, H.; Kim, T. H.; Kim, M. O. Protective effects of Anthocyanins against Amyloid beta-induced neurotoxicity in vivo and in vitro. *Neurochem. Int.* **2015**, *80*, 51–59.
- (3) Česonienė, L.; Jasutienė, I.; Šarkinas, A. Phenolics and anthocyanins in berries of European cranberry and their antimicrobial activity. *Medicina* **2009**, *45*, 992.
- (4) Steed, L. E.; Truong, V. D. Anthocyanin Content, Antioxidant Activity, and Selected Physical Properties of Flowable Purple-Fleshed Sweetpotato Purees. *J. Food Sci.* **2008**, *73*, S215–S221.
- (5) Salehi, B.; Sharifi-Rad, J.; Cappellini, F.; et al. The Therapeutic Potential of Anthocyanins: Current Approaches Based on Their Molecular Mechanism of Action. *Front. Pharmacol.* **2020**, *11*, 1300.
- (6) Wang, J.; Ho, L.; Zhao, W.; et al. Grape-derived polyphenolics prevent A β oligomerization and attenuate cognitive deterioration in a mouse model of Alzheimer's disease. *J. Neurosci.* **2008**, *28*, 6388–6392.
- (7) Liu, W.; Zhang, X.; Siems, W. F.; Hill, H. H.; Yin, D. Rapid profiling and identification of anthocyanins in fruits with Hadamard transform ion mobility mass spectrometry. *Food Chem.* **2015**, *177*, 225–232.
- (8) Laphorn, C.; Pullen, F.; Chowdhry, B. Z. Ion mobility spectrometry-mass spectrometry (IMS-MS) of small molecules: Separating and assigning structures to ions. *Mass Spectrom. Rev.* **2013**, *32*, 43–71.

- (9) Corinti, D.; Maccelli, A.; Crestoni, M. E.; et al. IR ion spectroscopy in a combined approach with MS/MS and IM-MS to discriminate epimeric anthocyanin glycosides (cyanidin 3-O-glucoside and -galactoside). *Int. J. Mass Spectrom.* **2019**, *444*, No. 116179.
- (10) Garcia-Oliveira, P.; Pereira, A. G.; Fraga-Corral, M.; et al. Identification, Quantification, and Method Validation of Anthocyanins. *Chem. Proc.* **2021**, *5*, 43.
- (11) Pachulicz, R. J.; Yu, L.; Jovcevski, B.; Bulone, V.; Pukala, T. L. Polyphenol characterisation and diverse bioactivities of native Australian lilly pilly (*Syzygium paniculatum*) extract. *Food Funct.* **2022**, *13*, 8585–8592.
- (12) Truong, V. D.; Deighton, N.; Thompson, R. T.; et al. Characterization of anthocyanins and anthocyanidins in purple-fleshed sweetpotatoes by HPLC-DAD/ESI-MS/MS. *J. Agric. Food Chem.* **2010**, *58*, 404–410.
- (13) Hong, H. T.; Netzel, M. E.; O'Hare, T. J. Optimisation of extraction procedure and development of LC–DAD–MS methodology for anthocyanin analysis in anthocyanin-pigmented corn kernels. *Food Chem.* **2020**, *319*, No. 126515.
- (14) Wu, X.; Prior, R. L. Identification and Characterization of Anthocyanins by High-Performance Liquid Chromatography–Electrospray Ionization–Tandem Mass Spectrometry in Common Foods in the United States: Vegetables, Nuts, and Grains. *J. Agric. Food Chem.* **2005**, *53*, 3101–3113.
- (15) Delgado-Povedano, M. D. M.; Villiers, A. D.; Hann, S.; Causon, T. Identity confirmation of anthocyanins in berries by LC-DAD-IM-QTOFMS. *Electrophoresis* **2021**, *42*, 473–481.
- (16) Stow, S. M.; Kurulugama, R. T.; Stafford, G. C.; et al. *Achieving Highly Accurate CCS Measurements in LC-IM-MS Analyses. Poster by Agilent Technologies*, Published 2018. Accessed January, 2023. https://www.agilent.com/cs/library/posters/public/AGILENT_ASMS2018_TP431.pdf
- (17) Stow, S. M.; Causon, T. J.; Zheng, X.; et al. An Interlaboratory Evaluation of Drift Tube Ion Mobility-Mass Spectrometry Collision Cross Section Measurements. *Anal. Chem.* **2017**, *89*, 9048–9055.
- (18) Ahmadiani, N.; Robbins, R. J.; Collins, T. M.; Giusti, M. M. Anthocyanins Contents, Profiles, and Color Characteristics of Red Cabbage Extracts from Different Cultivars and Maturity Stages. *J. Agric. Food Chem.* **2014**, *62*, 7524–7531.
- (19) Scalzo, R.; Genna, A.; Branca, F.; Chedin, M.; Chassaingne, H. Anthocyanin composition of cauliflower (*Brassica oleracea* L. var. botrytis) and cabbage (*B. oleracea* L. var. capitata) and its stability in relation to thermal treatments. *Food Chem.* **2008**, *107*, 136–144.
- (20) Wiczowski, W.; Szawara-Nowak, D.; Topolska, J. Red cabbage anthocyanins: Profile, isolation, identification, and antioxidant activity. *Food Res. Int.* **2013**, *51*, 303–309.
- (21) Charron, C. S.; Clevidence, B. A.; Britz, S. J.; Novotny, J. A. Effect of dose size on bioavailability of acylated and nonacylated anthocyanins from red cabbage (*Brassica oleracea* L. var. capitata). *J. Agric. Food Chem.* **2007**, *55*, 5354–5362.
- (22) Arapitsas, P.; Sjöberg, P. J. R.; Turner, C. Characterisation of anthocyanins in red cabbage using high resolution liquid chromatography coupled with photodiode array detection and electrospray ionization-linear ion trap mass spectrometry. *Food Chem.* **2008**, *109*, 219–226.
- (23) Kurulugama, R.; Imatani, K. *The Agilent Ion Mobility Q-TOF Mass Spectrometer System. Technical overview by Agilent Technologies*, Published February, 2021. Accessed December, 2022. <https://www.agilent.com/cs/library/technicaloverviews/public/S991-3244EN.pdf>
- (24) Zhu, P.; Tian, Z.; Pan, Z.; Feng, X. Identification and quantification of anthocyanins in different coloured cultivars of ornamental kale (*Brassica oleracea* L. var. acephala DC). *J. Horticult. Sci. Biotechnol.* **2018**, *93*, 466–473.
- (25) Sun, J.; Xiao, Z.; Lin, L. Z.; et al. Profiling polyphenols in five brassica species microgreens by UHPLC-PDA-ESI/HRMSn. *J. Agric. Food Chem.* **2013**, *61*, 10960–10970.